SUPPORTING INFORMATION

for the paper

Crystal engineering in two dimensions: an approach to molecular nanopatterning

Krishna G. Nath, Oleksandr Ivasenko, Jennifer M. MacLeod, Jill A. Miwa, James D. Wuest, Antonio Nanci, Dmitrii F. Perepichka and Federico Rosei

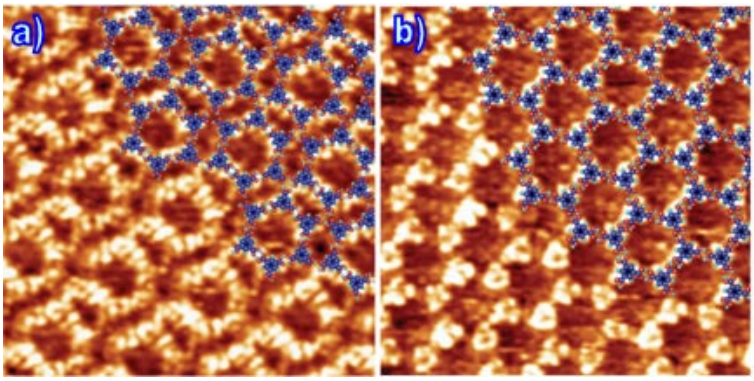

Figure S1. STM images and molecular models of 2D-SAMNs formed from TMA at the heptanoic acid/HOPG interface. (a) Flower structure (tunneling parameters: V_s = –0.95 V, I_t = 250 pA). (b) Chicken wire structure (tunneling parameters: V_s = –0.95 V, I_t = 200 pA). Both images are 10×10 nm^2.

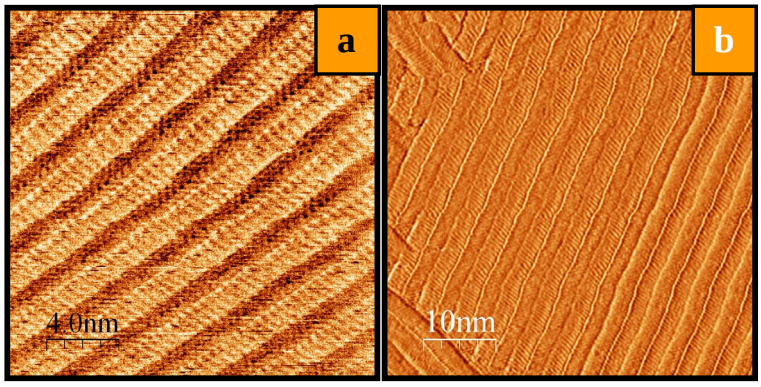

Figure S2. STM images of alcohol-only SAMNs formed from the alcohol-TMA mixture, in the absence of an appropriate solvent. (a) TMA/$C_{10}H_{21}OH$ mixture; (b) TMA/$C_{22}H_{45}OH$/ tridecane mixture. Tunneling parameters: I_t = 300 pA, V_s = –1200 mV (a), I_t = 289 pA, V_s = –1060 mV (b).

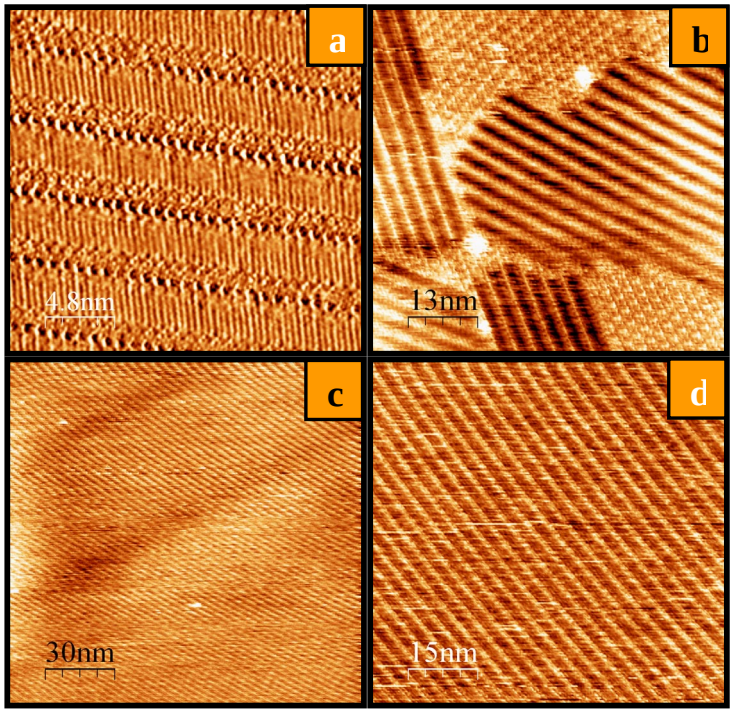

Figure S3. STM image of TMA/alcohol SAMNs formed in different solvents. (a) 1,2,4-trichlorobenzene (TMA/$C_{22}H_{45}OH$), (b) hexanoic acid (TMA/$C_{16}H_{33}OH$), (c) propionic acid (TMA/$C_{16}H_{33}OH$), (d) nonanoic acid (TMA/$C_{16}H_{33}OH$). Tunneling parameters: I_t = 300 pA, V_s = –1100 mV (a), I_t = 300 pA, V_s = –1600 mV (b), I_t = 300 pA, V_s = –1600 mV (c), I_t = 300 pA, V_s = –1200 mV (d).

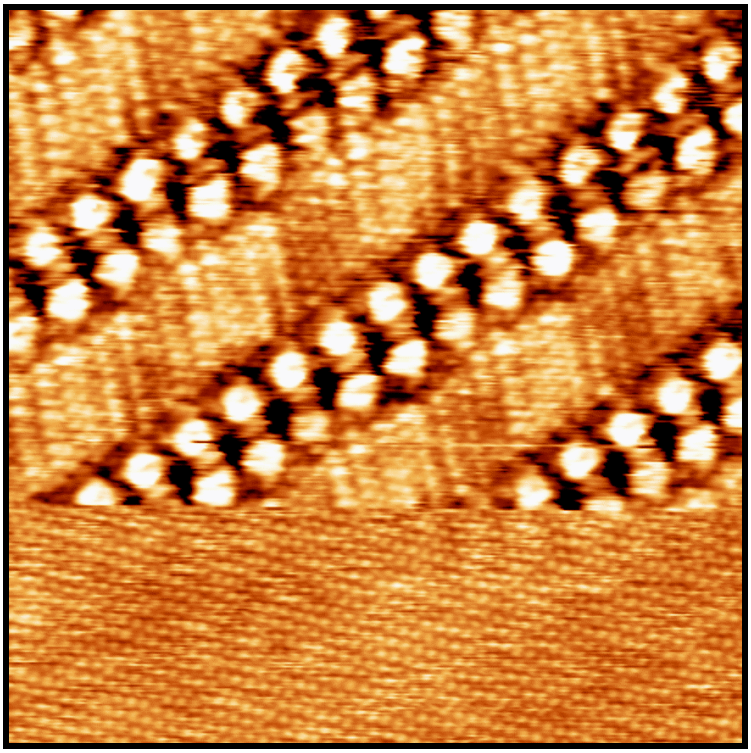

Figure S4. STM image of a TMA/$C_{17}H_{35}OH$ SAMN with the substrate HOPG imaged in the same frame, showing alcohol alignment along [01-20] zigzag direction of graphite. Image area 8.5 × 8.5 nm^2, I_t = 200 pA, V_s = –1600 mV (SAMN) and +200 mV (HOPG).

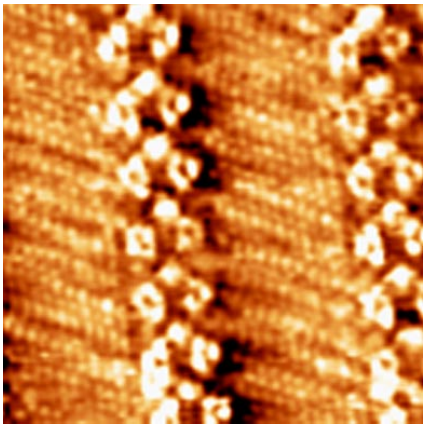

Figure S5. High-resolution STM images of TMA/1-Docosanol (C_{22}) SAMNs on HOPG, with an "unusual contrast" in the TMA tapes region. A bright protrusion is clearly seen in the cavity between the TMA dimers. Such contrast have been infrequently seen and are most likely is due to anomalous tip geometry or adsorption of unknown impurities. Image sizes: 7.5 × 7.5 nm^2. Tunneling parameters: V_s = –2.1V, I_t = 100pA.

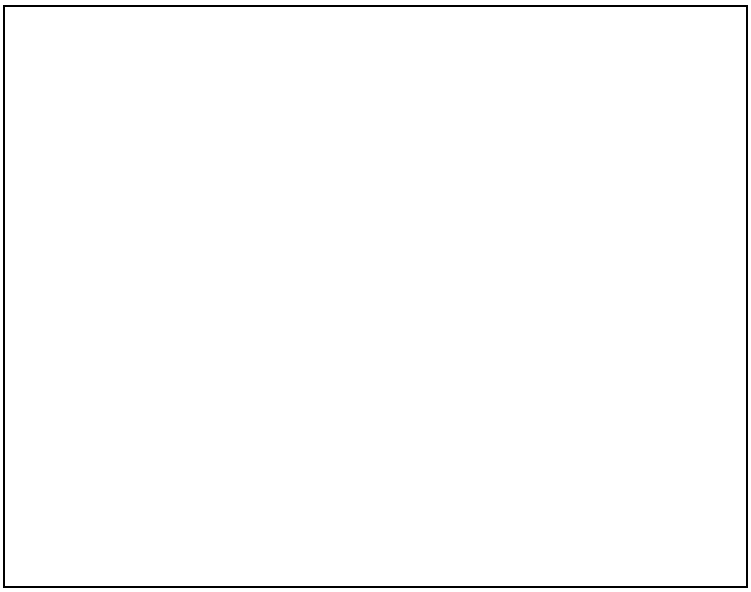

Figure S6. Average FFT for six line profiles taken along the "dimerized" alcohol lamellae in Fig. 8b. The profiles were taken parallel to the TMA dimer tapes. The FFT clearly shows that the dominant periodicity is at 0.96 nm, which corresponds to double the alcohol spacing. This supports the interpretation that the alcohols are dimerzed in this image. A smaller contribution at 0.48 nm arises due to the resolution of individual alcohols within the alcohol dimers.

Table S1. Results for B3LYP/6-31G(d,p) energy calculations for benzoic and trimesic acid and their hydrogen-bonded aggregates:

Entry	Molecule	Total Energy, Hartree	Total Energy, kcal/mol	Point group symmetry
A	H2O	-76.4197366	-47954.0725	C2v
B	PhCOOH	-420.835419	-264078.013	Cs
C	$(PhCOOH)_2$ [a]	-841.703367	-528176.438	Cs
D	$(PhCOOH)_3$ [a]	-1262.5480575	-792260.269	Cs
E	TMA	-797.9856321	-500743.166	C3h
F	$(TMA)_4$-$(H_2O)_2$ _ A [b]	-3344.9401666	-2098980.06	C2h
G	$(TMA)_4$-$(H_2O)_2$ _ B [b]	-3344.91228	-2098962.56	C2h
H	$(TMA)_4$-$(H_2O)_2$ _ C [b]	-3344.898969	-2098954.21	C2h

a) see Scheme 1 in the paper for the structure;
b) see Scheme 2 in the paper for the structure.

Hydrogen bonding enthalpy calculations:

ΔH ((PhCOOH)2) = C–2B = –20.4122 kcal/mol
ΔH ((PhCOOH)3) = C–3B = –26.2302 kcal/mol
ΔH ((TMA)4-(H2O)2 _ A) = F–4E–2A = –99.24996 kcal/mol
ΔH ((TMA)4-(H2O)2 _ B) = G–4E–2A = –81.75087 kcal/mol
ΔH ((TMA)4-(H2O)2 _ C) = H–4E–2A = –73.3981 kcal/mol

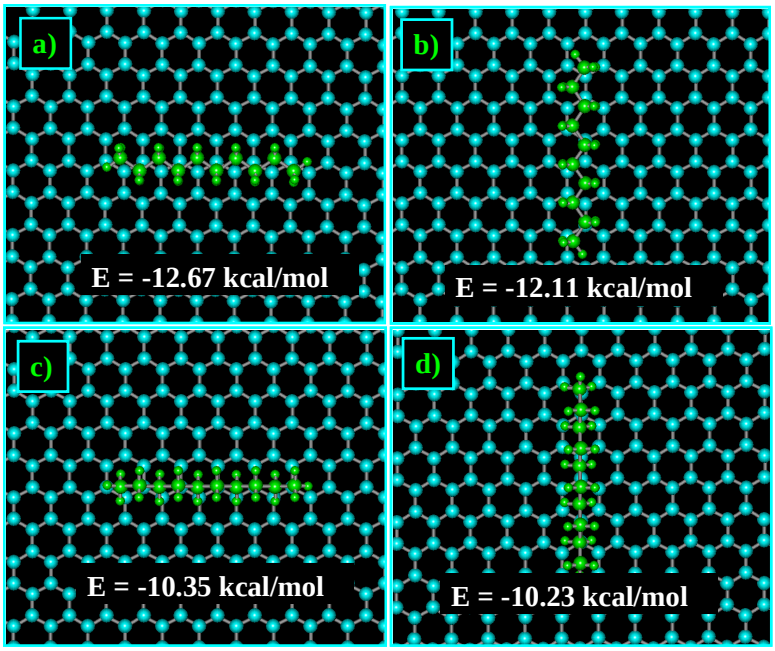

Figure S7. Molecular mechanics (MM+, Hyperchem 6) modeling of decane orientation on HOPG. Two energy minima are found: lower energy orientation along [01-20] zigzag direction (a,c) and higher energy orientation along [0010] armchair direction of graphene (b,d). The lower adsorption energy of alkyl chains coplanar with HOPG (a,b) compared to that of orthogonally oriented alkyl

chains (c,d) is predicted for chains with even number of carbons because in these only one of the two CH_3 groups can interact with HOPG in the orthogonal orientation.

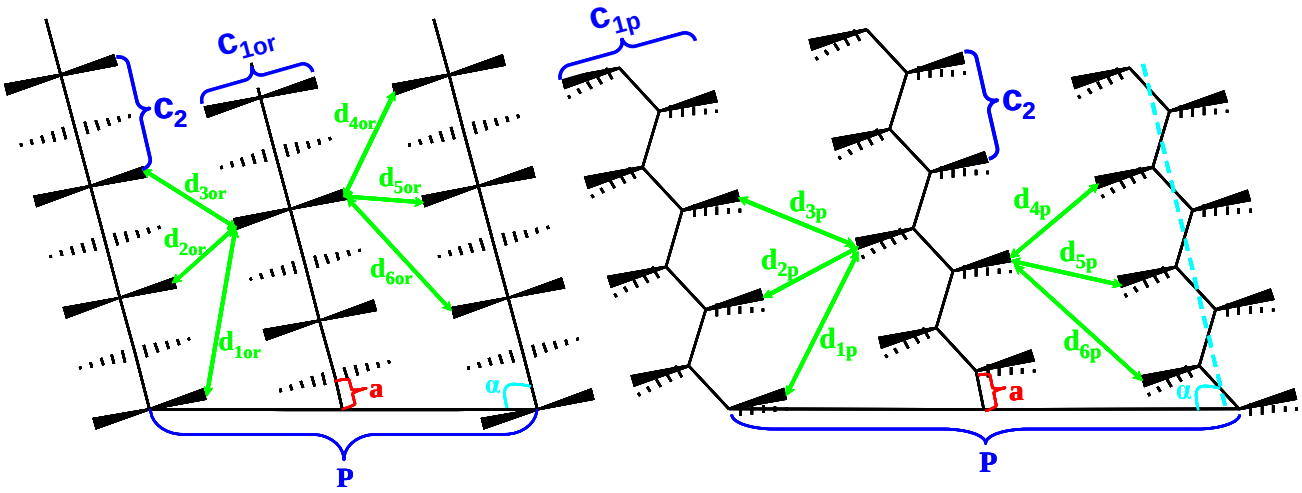

$$d_{1xx}=((0.5\cdot P\cdot \sin\alpha - c_{1xx})^2+(1.5\cdot c_2+a-0.5\cdot P\cdot\cos\alpha)^2)^{1/2}$$
$$d_{2xx}=((0.5\cdot P\cdot \sin\alpha - c_{1xx})^2+(0.5\cdot c_2+a-0.5\cdot P\cdot\cos\alpha)^2)^{1/2}$$
$$d_{3xx}=((0.5\cdot P\cdot \sin\alpha - c_{1xx})^2+(0.5\cdot c_2-a+0.5\cdot P\cdot\cos\alpha)^2)^{1/2}$$
$$d_{4xx}=((0.5\cdot P\cdot \sin\alpha - c_{1xx})^2+(1.5\cdot c_2-a-0.5\cdot P\cdot\cos\alpha)^2)^{1/2}$$
$$d_{5xx}=((0.5\cdot P\cdot \sin\alpha - c_{1xx})^2+(0.5\cdot c_2-a-0.5\cdot P\cdot\cos\alpha)^2)^{1/2}$$
$$d_{6xx}=((0.5\cdot P\cdot \sin\alpha - c_{1xx})^2+(0.5\cdot c_2+a+0.5\cdot P\cdot\cos\alpha)^2)^{1/2}$$

Figure S8. Description of the method for calculation of interchain H…H distances within alkane monolayer adsorbed on a flat surface. The calculations are done for an orthogonal (xx=or) and a parallel (xx=p) orientations of alkyl chains, with varied tilt angle (α) and relative shift of neighboring chains (a). C_{1or}, C_{1p} and C_2, are corresponding intrachain H…H distances (taken from semiempirical (AM1 models of n-decane) and P is a period of alkyl chains in the lamella. For the results of the calculations, see H-Hdistance.xls file.

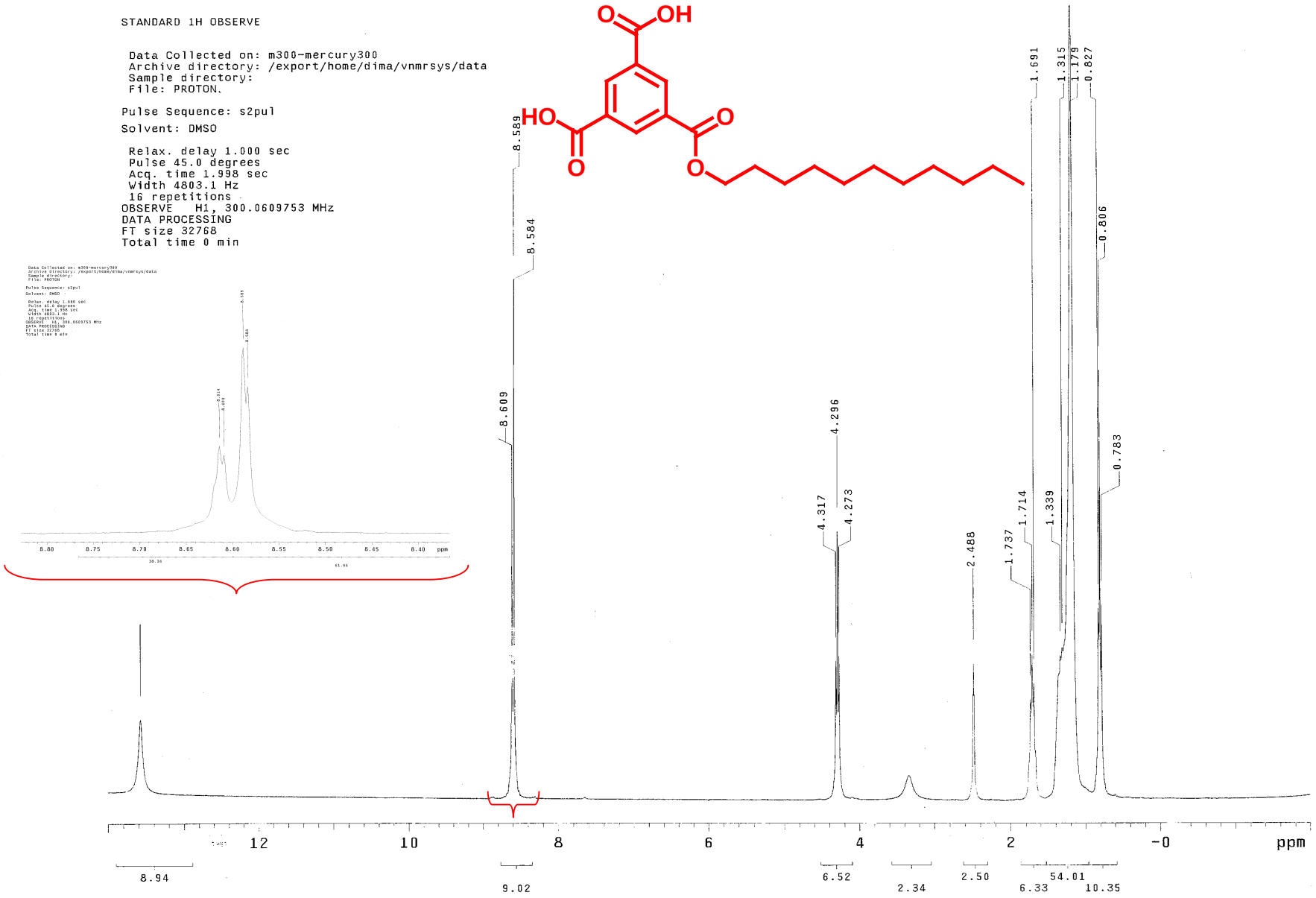

Figure S9. [1]H NMR of spectrum n-undecyl monoester of trimesic acid.

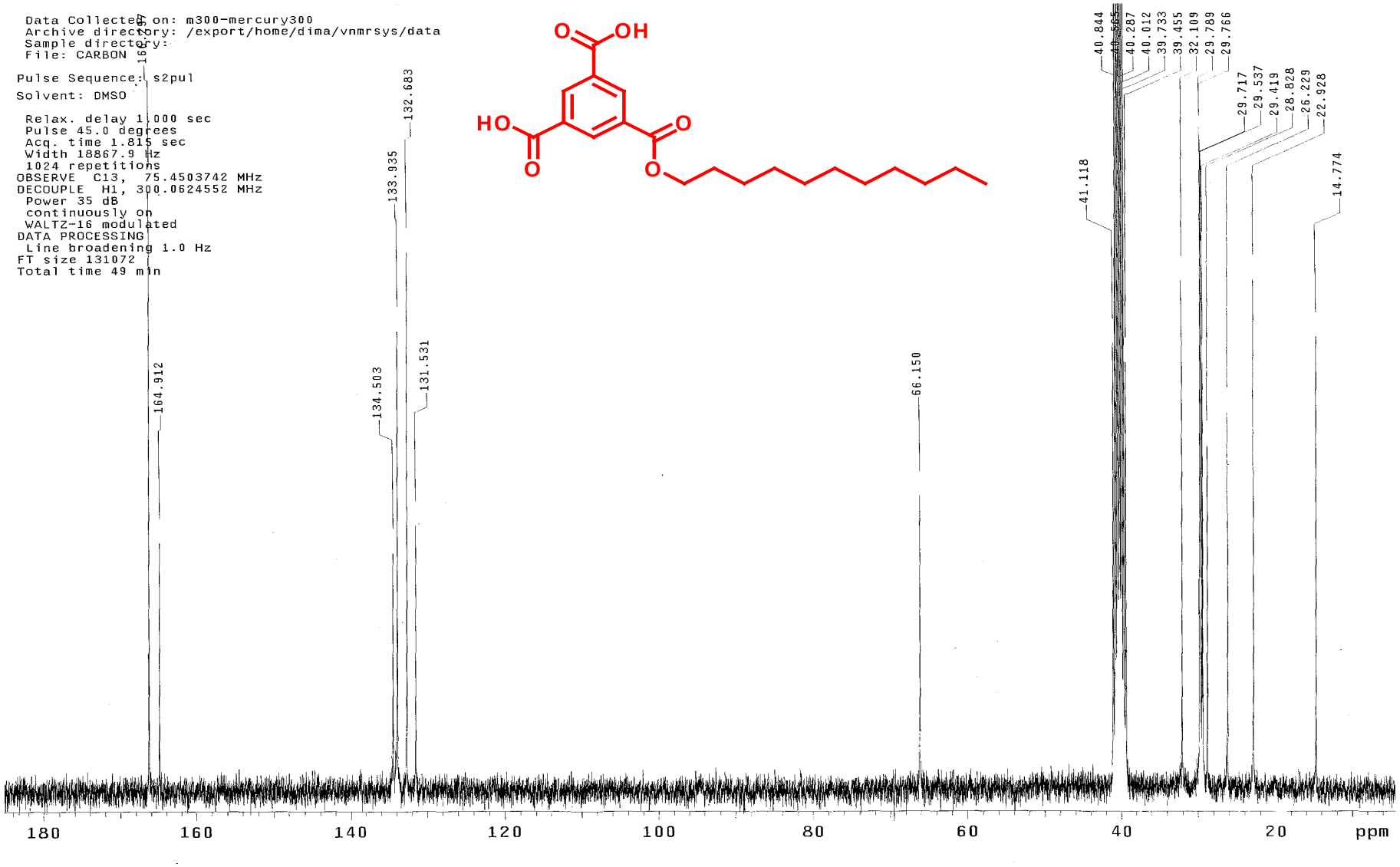

Figure S10. ^{13}C NMR spectrum of n-undecyl monoester of trimesic acid.

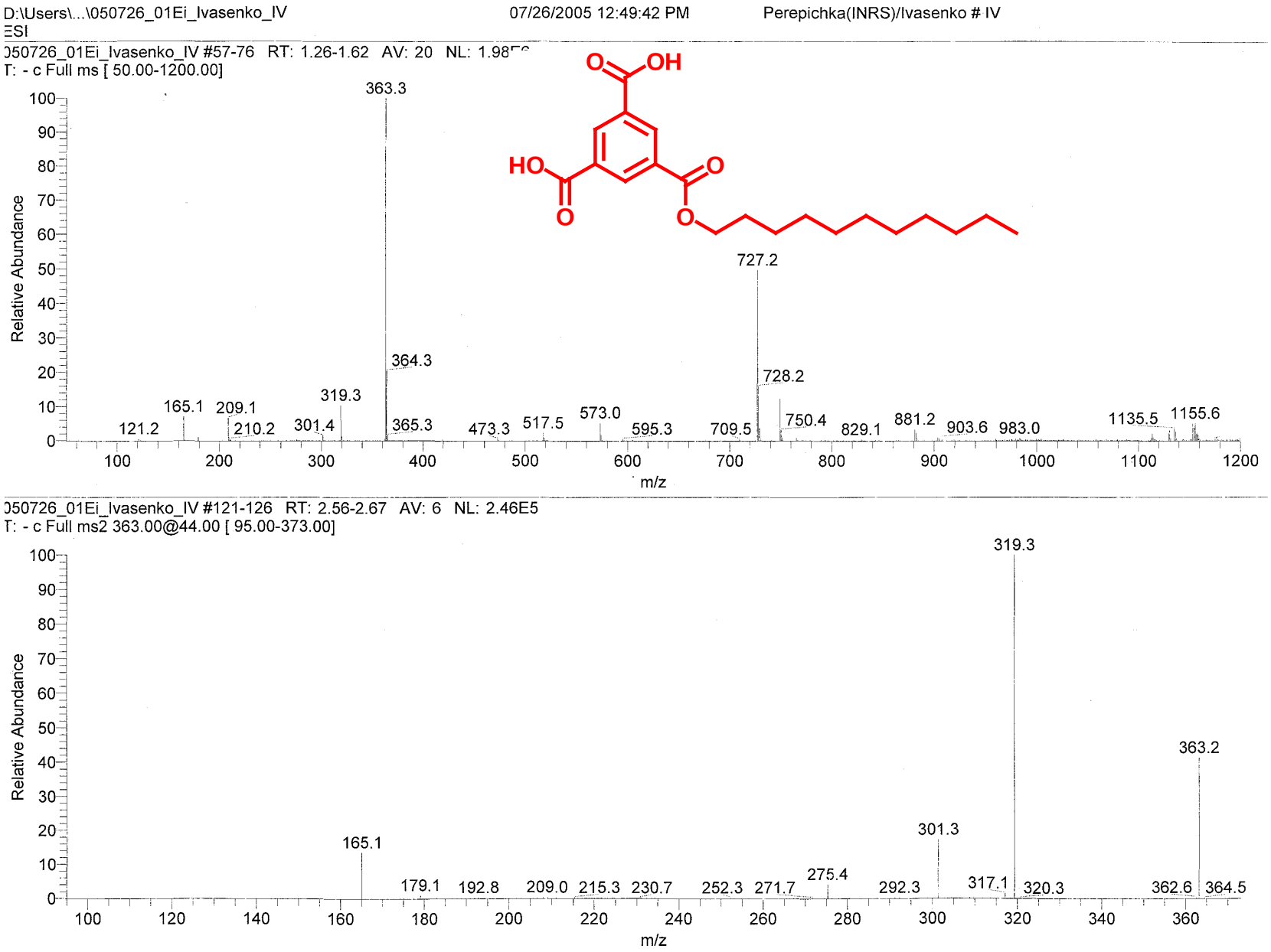

Figure S11. ESI (-) Mass spectrum of n-undecyl monoester of trimesic acid.

Full reference 57:

Gaussian 03, Revision D.01, Frisch, M. J.; Trucks, G. W.; Schlegel, H. B.; Scuseria, G. E.; Robb, M. A.; Cheeseman, J. R.; Montgomery, J. A.; Vreven, Jr. T.; Kudin, K. N.; Burant, J. C.; Millam, J. M.; Iyengar, S. S.; Tomasi, J.; Barone, V.; Mennucci, B.; Cossi, M.; Scalmani, G.; Rega, N.; Petersson, G. A.; Nakatsuji, H.; Hada, M.; Ehara, M.; Toyota, K.; Fukuda, R.; Hasegawa, J.; Ishida, M.; Nakajima, T.; Honda, Y.; Kitao, O.; Nakai, H.; Klene, M.; Li, X.; Knox, J. E.; Hratchian, H. P.; Cross, J. B.; Bakken, V.; Adamo, C.; Jaramillo, J.; Gomperts, R.; Stratmann, R. E.; Yazyev, O.; Austin, A. J.; Cammi, R.; Pomelli, C.; Ochterski, J. W.; Ayala, P. Y.; Morokuma, K.; Voth, G. A.; Salvador, P.; Dannenberg, J. J.; Zakrzewski, V. G.; Dapprich, S.; Daniels, A. D.; Strain, M. C.; Farkas, O.; Malick, D. K.; Rabuck, A. D.; Raghavachari, K.; Foresman, J. B.; Ortiz, J. V.; Cui, Q.; Baboul, A. G.; Clifford, S.; Cioslowski, J.; Stefanov, B. B.; Liu, G.; Liashenko, A.; Piskorz, P.; Komaromi, I.; Martin, R. L.; Fox, D. J.; Keith, T.; Al-Laham, M. A.; Peng, C. Y.; Nanayakkara, A.; Challacombe, M.; Gill, P. M. W.; Johnson, B.; Chen, W.; Wong, M. W.; Gonzalez, C.; Pople, J. A. Gaussian, Inc., Wallingford CT, 2004.